

# TECS Generalized Airplane Control System Design – An Update

Antonius A. Lambregts\*

**Abstract.** The Total Energy Control System (TECS) was developed in the early eighties to overcome well known safety/design deficiencies of traditional Single Input/Single output (SISO) based Flight Guidance and Control (FG&C) systems. TECS uses generalized Multi Input/Multi Output (MIMO) based airplane control strategies to functionally integrate all desired automatic and augmented manual control modes and achieve consistently high performance for airplane maneuvering in the vertical plane. This paper documents further insights gained over the past years on TECS design details for achieving precision control decoupling, integration of augmented manual control modes, embedded envelope protection functions and innerloop design using airplane dynamic model inversion. Additionally, non-linear design aspects are discussed, including thrust limiting, energy management, maneuver rate limiting and mode logic.

## 1 Introduction

Automatic Flight Guidance and Control (FG&C) systems have evolved into highly capable systems. These systems have contributed immensely to the improvement of aviation safety. Unfortunately, these systems still use traditional SISO control strategies that do not provide full 6 degrees of freedom airplane control. Therefore, airplanes equipped with these systems are still vulnerable to Loss of Control (LOC). Furthermore, these systems have become exceedingly complex, due to an excessive number of modes, mode overlap and mode idiosyncrasies, making it a challenge for the flight crew to avoid mistakes using these systems that can jeopardize operational safety. Most of the FG&C system modes are considered “non-flight critical”. This means that the flight crew is assumed to recognize and safely manage any failure of function of such modes. However, too often this assumption has proven to be unwarranted. As a result there have been too many automation related incidents and accidents, due to stall, roll divergence after an engine failure, icing etc. The current generation of FG&C systems do not take full advantage of modern MIMO control and functional integration strategies provide simpler, more efficient and less costly designs.

## TECS and THCS Development

FG&C system design and safety deficiencies were well recognized as long ago as the late seventies. In the early eighties NASA initiated research to address these deficiencies. This work resulted in the Total Energy Control System (TECS), which uses a generalized MIMO-based energy control strategy to functionally integrate all vertical flight path and speed control modes. This approach provides inherent envelope protection and avoids open ended SISO mode operations, thereby largely eliminating LOC safety risks. System complexities are reduced sharply by eliminating mode overlap, simplifying mode processing and providing more intuitive Man Machine Interfaces (MMI). Design generalization makes the system directly reusable, thereby reducing development costs for new applications. The system was successfully implemented and flight tested on the NASA B737 in 1985. The counterpart to TECS is the Total Heading Control System (THCS) which integrates all lateral directional control modes. Its design objectives and strategies are analogous to TECS. It was developed in the late eighties on the Condor High Altitude Long Endurance autonomous UAV program. TECS and THCS were successfully applied on the Condor and flight tested to demonstrate autonomous control capability under all operational and variety of failure conditions.

The basic TECS concepts are described in [1, 2]. This paper describes TECS design updates since the early nineties. A companion paper [3] describes design updates to the THCS design. It also describes a simplified TECS/THCS-based Mode Control Panel concept and a Primary Flight Displays concept that incorporates

---

\* Chief Scientific and Technical Adviser for Advanced Control

the TECS/THCS control and guidance strategies. Another companion paper [4] provides more details on Flight Envelope protection strategies.

**Design objectives.** The TECS/THCS design objectives include:

- use of *one* pilot-like MIMO-based control strategy for all automatic and manual control modes,
- full envelope protection to prevent LOC
- generalized functionally integrated design, consistency of operation between modes
- energy-efficient vertical flight path/speed control (elimination of stand-alone Autothrottle)
- decoupled Mode Command responses, reduced controller activity
- reduced design complexity by elimination of function overlap and using modular design
- simpler, more intuitive Mode Control Panel (MCP), clearer Flight Mode Annunciation (FMA)
- large cost reductions by generalized/reusable design, minimal application specific development, reduction in laboratory and flight testing and shorter application development cycle.

## 2 TECS –Architecture and Conceptual Design

### TECS Design

TECS uses a generalized MIMO based energy control strategy to provide all vertical flight path and airspeed control mode functions. Thrust is used to control the airplane's Total Energy requirement, the elevator is used to distribute the Total Energy between Potential and Kinetic energy.

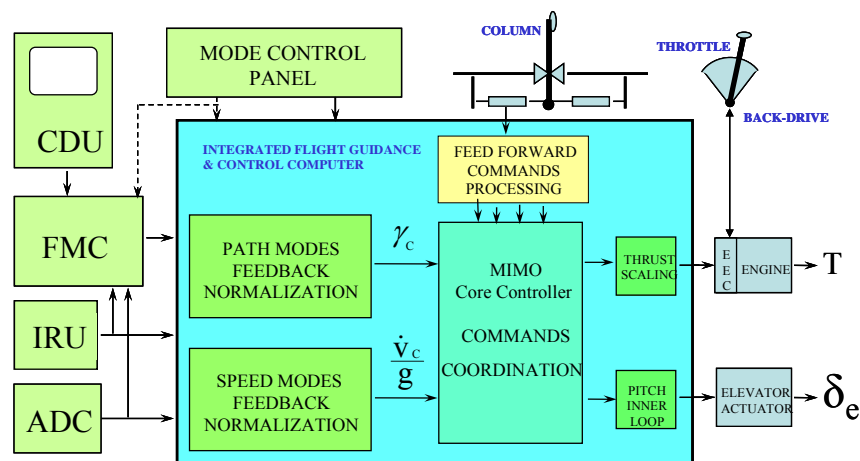


**Figure 2.1 TECS Architecture**

A detailed discussion about the energy based control and design generalization strategy can be found in [1]. The general architecture is shown in Figure 2.1

**Outerloop Modes Signal Processing.** The outerloop speed mode error is first converted to a true airspeed error and this error is multiplied by a factor  $K_v / g$  to produce the non-dimensional longitudinal acceleration signal ( $\dot{V}_c / g$ ). The outerloop path mode error (path deviation) is multiplied by a factor  $K_h / \hat{V}_{true}$  to produce the non-dimensional flight path angle signal ( $\gamma_c$ ). Speed and vertical path energy errors need to be weighted equally. Thus the gains  $K_v$  and  $K_h$  should have the same numerical value. The  $\dot{V}_c / g$  and  $\gamma_c$  signals are used as the standard inputs to the TECS Core Controller, see figure 2.1. The  $\hat{V}_{true}$  signal is a filtered true airspeed signal. This simple outerloop mode signal processing does not

include integral control signal paths to assure transient free mode switching and avoid the need for mode integrator initialization logic.

**Core Controller.** In the Core Controller the associated error signals  $(\dot{V}_\epsilon / g)$  and  $(\gamma_\epsilon)$  are formed. The sum of these error signals  $(\gamma_\epsilon + \dot{V}_\epsilon / g)$  represents the airplane's specific Total Energy Rate error signal. This signal is used in an integral control signal path, together with  $\hat{V} / g$  and  $\hat{\gamma}$  feedbacks used in proportional signal paths, to develop a normalized thrust command. Likewise, the difference between these error signals  $(\gamma_\epsilon - \dot{V}_\epsilon / g)$  represents the airplane's Differential Energy Rate error signal. In the original concept this signal was used in an integral control signal path, together with proportional  $\hat{V} / g$  and  $\hat{\gamma}$  feedback signal paths, to develop the elevator command during operations with the thrust command between Tmin and Tmax. In the current design, explained below,  $\gamma_\epsilon$  is used instead of  $(\gamma_\epsilon - \dot{V}_\epsilon / g)$  during operations with the thrust command between Tmin and Tmax. Because the error signals are used only in integral control signal paths, the control effectors respond to a step command from any of the outerloop modes with a control effector rate, resulting in smooth airplane dynamics.

**Avoiding outerloop mode tracking errors.** Since the integrators reside in the core controller, the feedback signals  $(\hat{\gamma}$  and  $\hat{V} / g)$ , used in the TECS Core Controller, must be re-referenced in the low frequency range to the outerloop mode true airspeed and vertical path feedback signals respectively, to avoid possible outerloop mode command tracking offset due to bias errors in these feedback signals. This is done by using free running complementary filters, designed to take into account turbulence and windshear effects on system performance.

**Command Response Decoupling.** In order to achieve decoupled outerloop command responses, *the Core Controller must be designed so that in response to a  $\dot{V}_c / g$  or a  $\gamma_c$  command, the  $(\gamma_\epsilon + \dot{V}_\epsilon / g)$  and  $(\gamma_\epsilon - \dot{V}_\epsilon / g)$  quantities go to zero simultaneously with identical dynamics.*

**Speed Envelope Protection – automatic modes.** Generally, for most automatic mode operations, whenever the thrust command is at the upper or lower limit, a *Speed-on-Elevator Control Priority (SoECP)* is used to maintain the commanded airspeed. For those cases there is no need for separate speed envelope protection functions. However, for the Glide Slope mode a *Path-on Elevator Control Priority (PoECP)* strategy is used to handle conditions with thrust command at the upper or lower limit. This strategy assures the Glide Slope will be captured when the airplane is at the correct position to do so, often while the thrust is at idle. Momentary open loop speed responses are protected by the Vmin and Vmax control. Vmin/Vmax and Normal Load factor protection is also provided as an integrated part of the augmented manual control modes and are used to protect automatic mode operations for such rare events.

**Normal Load Factor Protection - automatic modes.** In the original TECS design, normal acceleration limiting was achieved by placing a rate limiting function on the  $\gamma_c$  and  $\dot{V}_c / g$  signals. These rate limiting circuits introduce new system states which must be initialized at mode engagement and at any time the input to the rate limiter reverses direction, in order to avoid a response delays. To avoid this extra complexity an alternate method for normal load factor limiting, using amplitude limiting on  $(\gamma_\epsilon)$  and  $(\dot{V}_\epsilon / g)$  was developed. This method is described below.

**Energy Management during execution of simultaneous flight path and airspeed commands.** The rate limiters on the  $\gamma_c$  and  $\dot{V}_c / g$  signals (or the amplitude limiters on  $(\gamma_\epsilon)$  and

$(\dot{V}_e / g)$  signals in the updated design) also provide effective rate limiting on the thrust and elevator commands. In addition, these functions provide efficient airplane energy management during execution of large simultaneous vertical flight path and airspeed commands. If the commands have opposing energy demands, the  $(\dot{\gamma}_e)$  and  $(\dot{V}_e / g)$  error signal inputs to the TECS Core thrust control channel will initially cancel, so thrust will stay constant until the elevator control has exchanged kinetic energy and potential energy to the extent possible. This depends on the relative amplitude of the speed and flight path mode commands. After the energy exchange is completed a change in thrust will be commanded to reduce any remaining airplane total energy error to zero. Thus, thrust is always used efficiently.

If the commands require a substantial energy change in the same direction, the thrust command will quickly go the upper or lower limit with double the rate limit of a single command. After the thrust command reaches the limit, a **SoECP** will be used and a Control Authority Allocation (CAA) amplitude limit is applied to the  $(\dot{V}_c / g)$  signal. This CAA-limit, defined as  $(\dot{V}_c / g)_{\text{limit}} = K_{em}(\gamma + \hat{V} / g)$ , effectively limits energy rate used to execute the speed command. (The quantity  $(\gamma + \hat{V} / g)$  represents the airplane's total energy rate.) Therefore the remaining part of the available energy rate will by default be used to satisfy the flight path command. For example, if during a climb at maximum thrust and therefore  $(\gamma + \hat{V} / g) > 0$  a value of  $K_{em} = .5$  is selected, an accelerate command will be executed with half of the available energy rate. The other half is then allocated to continue the climb at ~half the initial rate. After the speed command is captured the climb rate will return to its original value, or if the altitude command is captured first, the acceleration will increase to capture the commanded speed, see the simulation results in Figure 3.7.

Similarly, if during idle descent when  $(\gamma + \hat{V} / g) < 0$  a value of  $K_{em} = 1$  is selected, a deceleration command temporarily reduce the climb rate to ~zero to capture the commanded speed and then the idle descent rate will be reestablished. This strategy facilitates the operational requirement for reducing the airplane speed to 250 knots or less, before descending below 10,000ft. In the original design, the required logic for this Energy Management function was complex and not without flaws. These flaws and the fixes developed are discussed below.

## TECS Performance in turbulence and windshear

Balancing the control command tracking performance and control effector activity for operation in turbulence and windshear conditions is a difficult problem for any flight control design. Reducing control effector activity inevitably results in deterioration of the command tracking in windshear. The performance objective used here for command tracking in a 1 knot/sec windshear is a peak IAS-error  $< 5$  knots and a vertical path deviation  $\Delta h < 20$  ft. The  $\hat{V}$ ,  $\hat{h}$ ,  $\hat{\alpha}$ ,  $\hat{\beta}$  filter gains are determined to achieve the preferred compromise between control effector activity in turbulence and reducing induced vertical and side acceleration and path deviation in windshear. It is beyond the scope of this paper to describe details related to choices of controller architecture, feedback signal processing and gains.

## 3 TECS -Design Updates

### Flight path and speed control decoupling - revisited

*From the start of the TECS and THCS development it has been a design objective to avoid ad hoc design and experimental tuning and instead use design solutions based on first principles of physics, whenever possible.* Since then a better theoretical insight has been gained into achieving improved decoupling of the flight path response from the execution of a speed command. In the original TECS concept the differential

energy rate error  $(\gamma_\epsilon - \dot{V}_\epsilon / g)$  was used as the input to the elevator control channel during operation with the thrust command between the lower and the upper limit. This conceptual architecture did not achieve the desired decoupling of the vertical path response during execution of an airspeed command. Therefore in the early TECS design an ad hoc method was used to improve path decoupling during speed command execution, with limited success. Later it was realized that an acceleration at constant flight path angle does not require an immediate change in pitch attitude, as is the case when changing flight path angle while maintaining airspeed. In fact, a permanent change in speed at 1 g flight requires a change in Angle of Attack and therefore an equal change in pitch attitude, which must be developed at the output of the integrator of the elevator control channel. Also, the change in angle of attack requires a change in the elevator trim, but this re-trim is accomplished in the updated design as part of the Short Period Model inversion, discussed below. Using this insight, the control strategy was changed from using  $(\gamma_\epsilon - \dot{V}_\epsilon / g)$  to using  $\dot{V}_\epsilon / g$  as the input to the elevator control channel, during operation with the thrust command between  $T_{min}$  to  $T_{max}$ . Also, a new  $\hat{V}_\epsilon / g$  signal with the gain  $K_{trim}$  is added to the input of the elevator control channel integrator, as shown in the revised Core Controller architecture of Figure 3.1, to retrim the pitch attitude command during speed changes.

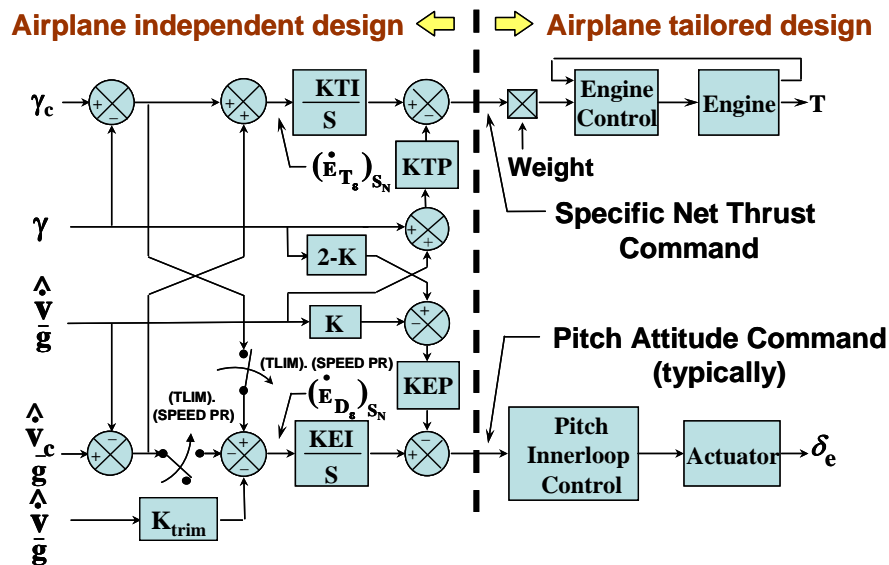


Figure 3.1 TECS Core Controller Architecture

Since the integral of  $(\hat{V}_\epsilon / g) \cdot K_{trim} \cdot KEI$  must equal the required change in pitch attitude, the value of  $K_{trim}$  is calculated using the 1 g relationship between Angle of Attack and true airspeed. Thus, it is found that  $K_{trim} = (1 / KEI) \cdot \{W / (\bar{q} \cdot S)\} / (C_{L\alpha} \cdot \hat{V}_{true})$ , where  $W$  = airplane weight,  $\bar{q}$  = dynamic pressure,  $S$  is the airplane wing reference area and  $C_{L\alpha}$  = lift coefficient change per unit angle of attack change. In addition, the proportional signal path through the gain  $KEP$  has been revised to now use  $\gamma$  only, at all times by selecting  $K=2$ , see next section below. These changes do not alter the energy redistribution nature of the elevator control, but do tend to favor suppression of path control tracking errors over speed control tracking errors in turbulence and windshear.

## TECS Core – Elevator Control Channel Design

**Classical approach.** The intent of the Energy Control strategy is to develop a priori coordinated thrust and elevator control commands, in order to decouple the outerloop flight path and speed command

responses. If this is realized, the elevator and thrust control channels can be treated as independent decoupled SISO components of the system. So, the elevator control channel can be designed using the Short Period airplane pitch dynamics Model Inversion, together with the simple first order representation of flight path angle response to pitch attitude. The thrust control channel design can also be approached as a simple “SISO” Energy Control problem.

During the early TECS development root locus analyses was used to define the Core Controller gains and gain schedules to support flight path and speed control modes at all flight conditions. This approach provides little or no physical insight into the reason why and how the gains need to change. A better approach to gain insight is to use first principles of physics, including Model Inversion, feedback concatenation/normalization, Control Bandwidth Separation or Pole Placement. These concepts are discussed below.

**Feedback Normalization/Concatenation, Pole Placement.** Consider figure 3.2, representing a plant model of 3 chained integrators, with concatenated feedback loops/gains closed around each plant state.

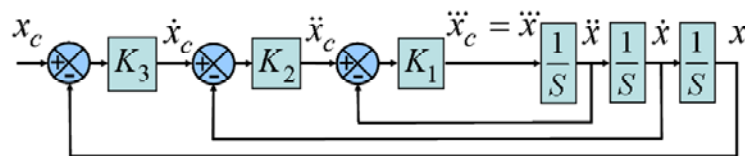


**Figure 3.2 Control Loop Concatenation**

The Transfer Function (TF) for this system is:

$$\frac{x}{x_c} = \frac{K_1 K_2 K_3}{S^3 + K_1 S^2 + K_1 K_2 S + K_1 K_2 K_3} \quad (3.1)$$

Note that the TF for a similar system with any number of concatenated system states can be written directly. The normalized loop gains relate directly to the physical properties of the controlled system, such as natural frequency and damping. Then, if the gain associated with each feedback loop, starting from the innermost loop, is dropped by a factor 4 or greater, the poles of the  $x/x_c$  transfer function will all fall on negative side of the real axis in a root locus plot. Alternatively, considering (3.1), it is easy to use Pole Placement to achieve the desired dynamics and find the required gains.

**Elevator control using Short Period Model Inversion.** *In our approach only the airplane rotational degrees of freedom are inverted.* The Short Period Model Inversion and rebuilding of the airplane pitch dynamics is shown figure 3.3. Note that pitch attitude ( $\theta$ ) can be used instead of Angle of Attack ( $\alpha$ ) to form the new desired pitch dynamics, as long as the frequency of the new augmented Short Period is selected to be in the frequency range where  $\theta \approx \alpha$ . Figure 3.3 does not show the pitching moment due to thrust, but this effect is included in the full design and analyses and simulations. The Model Inversion approach used here is not more risky than a classical design approach, since the same conservative gain and phase margins will be maintained to provide robustness against airplane model errors and unmodeled dynamics. *If the flight test results do not match the simulation results from the generalized control system design, there are only two possible causes: errors in the design implementation or, insufficient fidelity of the airplane and sensor models.* In that case it is more productive to correct possible design and implementation errors and, if necessary, develop higher fidelity airplane models, rather than revert to an ad hoc “trial and error” approach. The resulting new Short Period dynamics are represented by the TF:

$$\frac{\theta}{\theta_c} = \frac{K_q K_\theta}{S^2 + K_q S + K_q K_\theta} \quad (3.2)$$

To provide the proper flight path angle control dynamics to support closing of the outerloop mode

feedback, proportional  $\gamma$  feedback and integral control signal path of  $\gamma_\epsilon$  are closed around the  $\gamma/\theta_c$  transfer function, as shown in Figure 3.4.

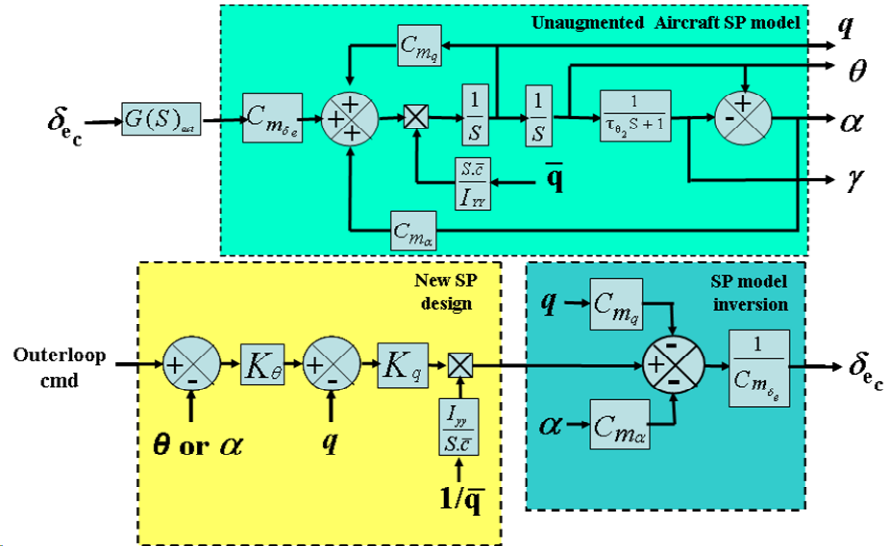


**Figure 3.3 Short Period Model Inversion and build up of new Short Period Dynamics**

The  $\gamma_c$  coming from the automatic, or the augmented manual mode which develops  $\gamma_c$  by integration of the vertical control inceptor signal ( $\delta_{vci}$ ). [An alternate architecture using ( $\gamma_\epsilon$ ) in the proportional signal path has also been developed [6], but this architecture has disadvantages for the automatic control modes.] The controller structure of figure 3.4 was specifically developed to support the manual mode bandwidth requirement, by using pole zero cancellation to create effectively a lower order [ $\gamma / \delta_{vci}$ ] TF, as explained in section 4, below.

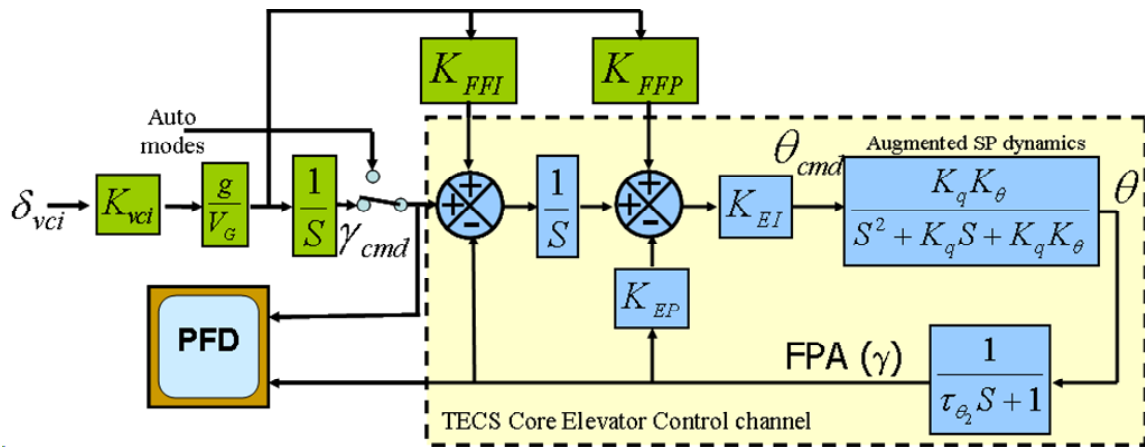


**Figure 3.4 TECS Core elevator control channel**

To make this possible the  $[\gamma / \theta]$  heave dynamic have been made to appear as an explicit part of the  $[\gamma / \gamma_c]_{auto}$  TF. By selecting  $K_{EP} = \tau_{\theta_2}$  the TF for the automatic modes becomes ( $K_{FFI}$  and  $K_{FFP}$  both set to zero):

$$\left[ \frac{\gamma}{\gamma_c} \right]_{auto} = \frac{\theta}{\gamma_c} \cdot \frac{\gamma}{\theta} = \frac{1}{[ \{1 / (K_q \cdot K_\theta \cdot K_{EI})\} S^3 + \{1 / (K_\theta \cdot K_{EI})\} S^2 + (1 / K_{EI}) S + 1 ] (\tau_{\theta_2} S + 1)} \quad (3.3)$$

Note that the variation of  $\tau_{\theta_2}$  no longer affects the system stability. The heave time constant is defined as:

$$\tau_{\theta_2} = \frac{C_L \cdot V_{true}}{g \cdot C_{L\alpha}} = \frac{W \cdot V_{true}}{g \cdot C_{L\alpha} \cdot \bar{q} \cdot S} \quad (3.4)$$

This  $\tau_{\theta_2}$  can be readily computed/updated by the onboard flight control computer.

**Normal Load Factor limiting – Revisited.** Using  $\gamma_\varepsilon$  instead of the  $(\gamma_\varepsilon - \dot{V}_\varepsilon / g)$  as the input to the elevator control channel during operations with the thrust between the lower and upper limit also solved a Normal Load Factor (NLF) control issue. In the earlier design, during execution of simultaneous  $\dot{V}_c / g$  and  $\gamma_c$  with opposite signs, the effective Normal Load Factor limit was twice the intended value, because **both**  $\dot{V}_c / g$  and  $\gamma_c$  contributed to the effective NLF-limit. The new control strategy, using **either**  $\gamma_\varepsilon$  or  $\dot{V}_\varepsilon / g$ , eliminates this problem. As mentioned above, in the current design NLF control for the automatic modes is achieved by placing an amplitude limit on the  $\gamma_\varepsilon$  and  $\dot{V}_\varepsilon / g$  signals. This amplitude limit is calculated as follows. Given a  $NLF_{limit}$ , the normal acceleration limit is  $g \cdot NLF_{limit}$ . So the desired flight path angle rate limit becomes  $\dot{\gamma} = NLF_{limit} \cdot g / V_G$ . According to (3.3) for a ramping  $\gamma_c$  the flight path angle response will lag the command by an amount:

$$\tau_\gamma = 1 / KEI + \tau_{\theta_2} \quad (3.5)$$

Then,  $\gamma_\varepsilon = \tau_\gamma \cdot \dot{\gamma}$ . Therefore the amplitude limit on  $\gamma_\varepsilon$  should be:

$$\gamma_{\varepsilon_{limit}} = (NLF_{limit} \cdot g / V_G) (1 / KEI + \tau_{\theta_2}) \quad (3.6)$$

Also, the same limit needs to be applied to the  $\dot{V}_\varepsilon / g$  signal, to achieve the same NLF control during operations with **SoECP** when the thrust command is at the upper or lower limit.

When the  $\gamma_\varepsilon$  or the  $\dot{V}_\varepsilon / g$  signal at its limit, the feedback path to the integrator is effectively broken, so it must be shown that the remaining elevator/thrust control configuration maintains satisfactory  $\gamma$  and  $\Delta T$  response dynamics.

## TECS Core - Thrust Control Channel Design

The basic control decoupling requirement is met when the responses of  $(\gamma_\varepsilon - \dot{V}_\varepsilon / g)$  and  $(\gamma_\varepsilon + \dot{V}_\varepsilon / g)$  due to a  $\gamma_c$  or a  $\dot{V}_c / g$  command are identical. The equation for  $\Delta T_{required}$  is:

$$\Delta T_{required} = W \cdot (\Delta \gamma + \dot{V} / g) + \Delta Drag \quad (3.7)$$

It can be shown that during automatic mode operations the drag change due to incremental NLF (which is limited to .1 g), can be neglected. From this equation it follows that ideally, in order to maintain  $\dot{V}_\varepsilon / g = 0$  during the execution of a  $\gamma_c$  maneuver, the following TF identity must hold:

$$[(\Delta T / W) / \gamma_c]_{thrust} = [\gamma / \gamma_c]_{elevator} \quad (3.8)$$



Then by inference, in order to maintain  $\gamma_\varepsilon = 0$  during execution of an acceleration command, the following TF identity will hold too:

$$[(\Delta T / W) / (\dot{V}_c / g)] = [(\Delta T / W) / \gamma_c] \quad (3.9)$$

The above decoupling requirements can be achieved by matching thrust control channel dynamics to mimic the elevator control channel dynamics. One approach is to select  $K_{TI} = K_{EI}$  and  $K_{TP} = K_{EP}$ , and insert a matching filter before the final Thrust Command that represents the augmented pitch attitude and heave dynamics, as well as the inverted engine dynamics  $[1 / (T / T_c)]$ . This approach and also another more traditional approach, matching the TF frequency/amplitude responses, were evaluated. Both approaches produced very good control decoupling results. However, the more traditional design resulted in a simpler design and achieved slightly better decoupling of the flight path and airspeed command responses. It also resulted in much lower gains  $K_{TP}$  and  $K_{TI}$  and therefore lower control activity in turbulence. Simplicity has its advantages.

## Provisions for Thrust and Elevator Command saturation

The classical way to limit the final thrust command is to continually calculate and apply the integrator limit by subtracting the contribution of the proportional  $(\gamma + \hat{V} / g)$  signal path from the externally provided Net Thrust Limit (NTL). Alternatively, the integrator may be moved to end of the net thrust command signal processing path, where its output can be simply limited to the engine's net thrust command limit, provided by the FADEC. In that case, a differentiator function must be placed in the proportional  $(\gamma + \hat{V} / g)$  signal path. In the later TECS designs the latter approach is used, because it is simpler.

Likewise, similar provisions must be implemented to prevent windup of the integrator in the elevator command processing signal path.

## Priority use of Elevator when the thrust command is at a limit

The change to using  $\gamma_\varepsilon$  instead of  $(\gamma_\varepsilon - \dot{V}_\varepsilon / g)$  as the input to the TECS Core elevator control channel during MIMO control, allowed the elevator control priority logic for conditions with thrust at the upper or lower limit to be simplified considerably. It also allows smooth, transient-free execution of simultaneous airspeed and flight path commands for all possible combinations of amplitude and timing to be achieved. The updated Elevator Control Priority works as follows. When the thrust command is within the linear control range between Tmin and Tmax, Path-on-Elevator Control Priority (**PoECP**) is used. **PoECP** also remains in effect after the thrust command reaches Tmax or Tmin when  $\gamma_c \leq .5(\hat{\gamma} + \hat{V} / g)$  and one of the following modes is engaged:

- the FPA mode, or
- the Altitude Acquisition/Hold mode, or
- the Glide Slope mode, or
- the Augmented Manual control mode, and the control inceptor is at neutral
- the Augmented Manual control mode, and the control inceptor is deflected and the Vmin/Vmax envelope protection control priority is not in effect

Using **PoECP** during operation in the Altitude Acquisition/Hold mode or the Glide Slope control mode when the thrust command is at the upper or lower limit is self evident. In that case the airplane will stay on the commanded flight path and accelerate/decelerate according to the available "excess energy rate". This strategy assures that the Glide Slope will be captured, when the airplane is at the right position for capture, either from below or from above the glide slope. When the thrust command reaches Tmin or Tmax, Speed-on-Elevator Control Priority (**SoECP**) is invoked in the following situations:

- Altitude Acquisition or FPA mode engaged and  $T_c = T_{\max}$  and  $\gamma_c > K_{ECP} \cdot (\hat{\gamma} + \hat{V} / g)$ , or
- Altitude Acquisition or FPA mode engaged and  $T_c = T_{\min}$  and  $\gamma_c < K_{ECP} \cdot (\hat{\gamma} + \hat{V} / g)$ , or
- Augmented Manual Control mode engaged and the control inceptor is at neutral, or
- Augmented Manual Control mode engaged and the control inceptor is not at neutral and either the Vmin control develops a more nose down command than the Manual FPA Control mode, or the Vmax control develops a more nose up command than the Manual FPA Control mode.

Currently,  $K_{ECP} = .5$  has been selected. When  $\gamma_c > K_{ECP} \cdot (\hat{\gamma} + \hat{V} / g)$  is not true (for small values of  $\gamma_c$ ) speed commands will be executed using **PoECP**, e.g. when the Altitude Hold mode is engaged, or during a shallow climb in the FPA mode. When  $\gamma_c > K_{ECP} \cdot (\hat{\gamma} + \hat{V} / g)$  is true, then there would be little control authority to accelerate using the thrust only, so in that case the **SoECP** is invoked and part of the energy rate used for climbing is transferred to accelerate the airplane and capture the commanded speed quicker. Examples of Energy Management cases are shown in figure 3.7. When **SoECP** is invoked the  $\gamma_\epsilon$  signal input to the Core Controller is replaced with the  $\dot{V}_\epsilon / g$  signal, see figure 3.1. In that case, to allow for execution of a simultaneous flight path command, Control Authority Allocation (CAA) is applied to the longitudinal acceleration command ( $\dot{V}_c / g$ ). The CCA function is explained in more detail in the next section. Then, when the thrust command computation computes a thrust rate command that drives the thrust command out of the limit, the control priority reverts back to flight path control priority. The thrust coming off its limit always coincides with the start of the final flight path or speed command capture phase.

## Energy Management during execution of simultaneous flight path and airspeed commands – Revisited

In the earlier TECS design the Energy Management function and associated logic was rather complex and not without flaws. One of the reasons was that the differential energy rate error ( $\gamma_\epsilon - \dot{V}_\epsilon / g$ ) was used as the input to the elevator control channel during operations with the thrust command between Tmin and Tmax. When during the capture of a flight path command the thrust came off its limit, the Core elevator control channel would revert to using ( $\gamma_\epsilon - \dot{V}_\epsilon / g$ ) as its input signal. This made it difficult to smoothly capture smooth vertical path, if at that time the  $\dot{V}_\epsilon / g$  signal was not close to zero. The revised control priority logic discussed above, using **PoECP** during operations with the thrust command between Tmin and Tmax has made it possible to greatly simplify the Control Authority Allocation (CAA) associated signal processing. In the current design, the Core elevator control channel only uses the  $\dot{V}_\epsilon / g$  signal as its input when the SoECP is invoked. Therefore, in the current design, the  $\dot{V}_\epsilon / g$  signal that is routed the Core elevator control channel has the CCA amplitude limit [ $K_{em}(\gamma + \hat{V} / g)$ ] applied to it full time. No CCA amplitude limit is applied the  $\dot{V}_\epsilon / g$  signal that is routed the thrust control channel, so the thrust control channel always uses the basic ( $\gamma_\epsilon + \dot{V}_\epsilon / g$ ) signal. The CCA associated logic used in the earlier design has been eliminated.

## TECS Automatic Modes Simulation Results

**Simulation.** A complete TECS/THCS system simulation capability was developed in MATLAB-Simulink. The simulation includes all TECS and THCS modes and design features discussed above in this paper, as well as a full flight regime six degrees of freedom nonlinear airplane simulation. Realistic 2<sup>nd</sup> order actuator models including rate and position limits were included, along with a rate limited 2<sup>nd</sup> order

engine model. The system time responses below were generated using this simulation. No “design tuning” is used for any of the maneuvers shown below. The airplane model represents a generic 100-125 passenger twin turbofan engine transport airplane at 120,000 lbs.

**Results.** Figure 3.5 shows the airplane response to a 25 knots step command (left plot) and a 100 knots step command (right plot) in the IAS and Altitude Hold modes.

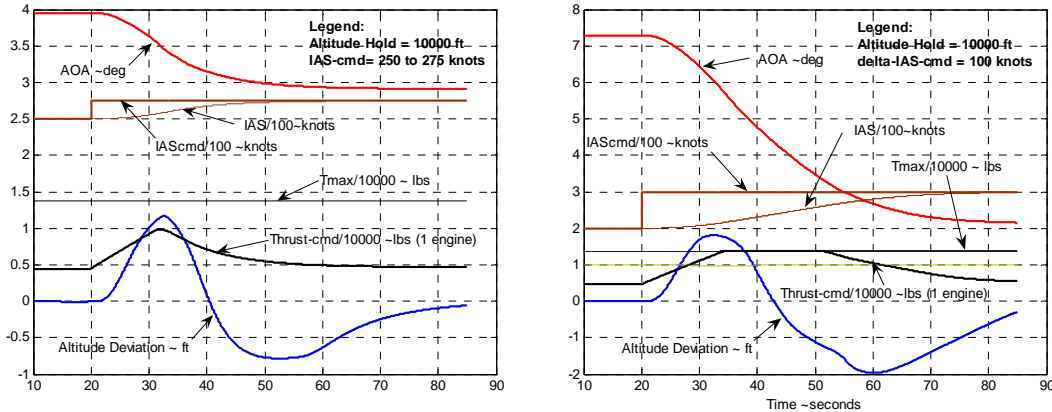


**Figure 3.5 TECS Responses to step IAS-cmd: 25knots (left), 100 knots (right)**

The responses are very smooth and the flight path coupling error due to the execution of the speed command is very small: the temporary altitude deviation was a little over 1 ft for the 25 knots speed increase (within the “linear” thrust operating range) and ~2 ft altitude deviation for the 100 knots speed change, which involved a 20 second period with the thrust command at the upper (Tmax) limit.

In Figure 3.6 the system responses are shown for the IAS and Altitude Acquisition modes for step altitude commands of 500 ft (left plot), and 5000 ft (right plot). For both cases the responses are smooth and without an overshoot of the command. For the 500ft step command case the thrust does not reach the limit (Tmax). For the 5000 ft step command case the thrust reaches Tmax and stays there for ~60 seconds before the thrust is reduced smoothly during the final linear exponential capture. There are no perceptible control transients resulting from the reversion from PoECP to SoECP and vice versa. In both cases the maximum speed deviation is limited to ~.2 knots. Notice also that the NLF is limited to .1 and that Tmax slowly decreases during the climb, due to the air density effect on the engine thrust.

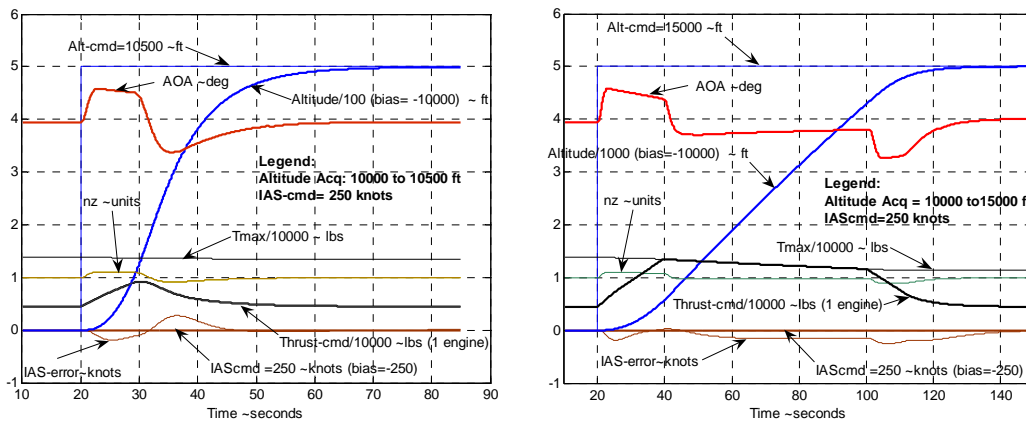


**Figure 3.6 Responses to step Altitude-cmd: 5500 ft (left), 5000ft (right)**

In **Figure 3.7 left plot**, the system responses are shown for the IAS and Altitude Acquisition modes for a step Alt-cmd = 3000 ft at t= 20 seconds and a step IAS-cmd = 100 knots at t=60 seconds.

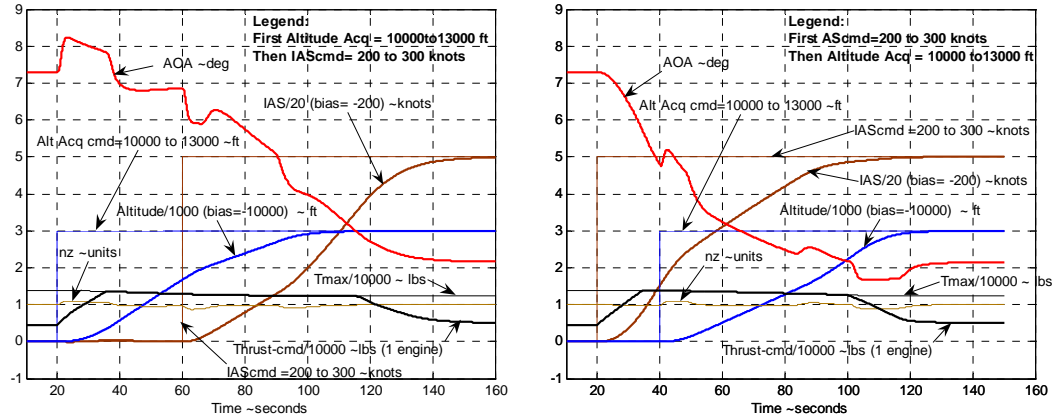


**Figure 3.7 Energy Management for Altitude Acquisition and IAS commands;**  
**Left: Alt Acq-cmd =10k to 13k ft at 20 sec; IAS-cmd = 200 to 300 knots at 60 sec;**  
**Right: IAS-cmd = 200 to 300 knots at 20 sec; Alt Acq-cmd =10k to 13k ft at 60 sec.**

The timing of the commands are chosen to demonstrate the “pilot like” Energy Management feature built into the system. The altitude command drives the thrust command to  $T_{max}$ , establishing **SoECP**. Then when the IAS-cmd follows, the Control Authority Allocation (CAA) limit,  $K_{em}(\hat{\gamma} + \hat{V} / g)$  with  $K_{em} = .5$ , is placed on the  $\dot{V}_c / g$  signal, causing the airplane to reduce the climb rate by ~50 % to execute the IAS-cmd. During the execution of the IAS-cmd the  $\gamma_c$  drops below  $.5(\hat{\gamma} + \hat{V} / g)$ , causing the elevator control priority to revert from **SoECP** to **PoECP**, allowing the ALT-cmd to be captured. At this point the Total Energy demand is not yet satisfied, so the thrust stays at  $T_{max}$  and the excess energy rate is now causing the acceleration to increase. Then, when the airspeed comes within the capture range, the thrust command drops below  $T_{max}$ , **PoECP** is reestablished and the commanded airspeed is captured exponentially.

In **Figure 3.7 right plot**, the system responses are shown for the same step Alt-cmd =3000 ft and IAS-cmd=100 knots, but order is reversed. Now the IAS-cmd causes the thrust to ramp up to  $T_{max}$ , to accelerate the airplane while maintaining **PoECP**, until at t=40 seconds the step Alt-cmd results in  $\gamma_c > .5(\hat{\gamma} + \hat{V} / g)$ , causing a reversal of the elevator control priority to **SoECP** with the CCA acceleration limit  $(\dot{V}_c / g)_{limit} = .5(\hat{\gamma} + \hat{V} / g)$  applied to the  $\dot{V}_c / g$  signal that is routed to the elevator control channel. This causes the acceleration to drop to  $\dot{V}_c / g = .5(\hat{\gamma} + \hat{V} / g)$ , thereby transferring ~50 % of the energy rate to the execution of the climb command, while maintaining  $T = T_{max}$ . Next, the IAS-cmd is captured first, but since at this point still  $\gamma_c > .5(\hat{\gamma} + \hat{V} / g)$  the **SoECP** is maintained. During the IAS-cmd capture, the excess energy is transferred to increase the climb rate, while maintaining  $T = T_{max}$ . When the thrust command drops below  $T_{max}$ , the “linear” **PoECP** capture of the Alt-cmd begins.

## 4 Flight Path Angle based Augmented Manual Control

### Specific design Objectives

The FBW Augmented Manual Control mode provides pilot maneuvering capability in the vertical plane by using the vertical control inceptors. A earlier stand-alone Flight Path Angle based augmented manual control mode was developed and flight demonstrated/evaluated under the NASA TCV Program 1976-79 [3]. Key design objectives include:

- good handling qualities at all flight conditions, with precision maneuvering capability
- reduced pilot workload using “Direct FPA Control” strategy , eliminating need for continuous compensatory pitch attitude control.
- carefree maneuvering capability to the limits of the safe airplane performance, using envelope protection to reduce the risk of Loss of Control (LOC)
- operational consistency with automatic modes, one pilot “mental model” for all operations
- clean and simple integration of the manual and automatic modes, shared function elements

In order to achieve the last three objectives the Augmented Manual control mode is designed as a simple augmentation to the automatic FPA control mode. Thus, the Core elevator control channel of figure 3.4 provides the basic airplane control when the pilot is not using the control inceptor. The airplane then maintains the last pilot-established earth referenced  $\gamma$ , regardless of changes in airspeed, airplane configuration changes or disturbances due to turbulence and windshear. As a result this FPA Rate Command Hold strategy largely eliminates the need for the pilot to use a **Continuous Compensatory Control Strategy**. Instead the control tracking performance tends to improve when the pilot adopts an **Intermittent Maneuver Control Strategy**. So, the main reasons for going to a “Direct FPA Control” strategy are to reduce the tedious kind of workload controlling flight path perturbations, and to simplify interception and tracking a vertical path in space. This operation can be further enhanced by proper flight displays, e.g. a HUD or Synthetic Vision background display of the airport and runway. This makes it easy to capture a desired Glide Path and from there on, the FPA-based Augmented manual control algorithm will track the pilot established flight path with little or no need for pilot corrections. This capability, then called “Velocity Vector Control”, was first developed and demonstrated by NASA under the TCV program in the late 1980-ties [5].

## Design Implementation

For the design shown in figure 3.4 the control inceptor command signal is processed in three very basic feed forward command paths. The first signal path integrates the inceptor command to establish the reference  $\gamma_c$ . The second and third signal paths shape the control responses of the airplane to achieve the exact response dynamics prescribed by a specified ideal (classical) handling qualities model. Briefly, the TECS Core elevator control channel  $[\gamma / \gamma_c]_{auto}$  TF, equation (3.3), has a unity numerator and a fourth order denominator. The feedback and feed forward gains of this Core Controller can be selected such that the resulting augmented manual  $[\gamma / \delta_{vci}]$  TF results in a  $[\theta / \delta_{vci}]$  TF that represents a specified ideal handling qualities model, for example:

$$\frac{\theta}{\delta_{vci}} = \frac{K_{vci}}{S} \frac{g}{V_G} \frac{(\tau_{\theta_2} S + 1) \omega_{SP}}{S^2 + 2\zeta_{SP} \omega_{SP} S + \omega_{SP}^2} \quad (4.1)$$

Here  $\delta_{vci}$  is the vertical control inceptor deflection,  $K_{vci}$  is the vertical control inceptor gain. Since

$$\frac{\gamma}{\delta_{vci}} = \frac{\theta}{\delta_{vci}} \frac{\gamma}{\theta} = \frac{\theta}{\delta_{vci}} \frac{1}{(\tau_{\theta_2} S + 1)} \quad (4.2)$$

it follows in order to achieve (4.1), the final  $[\gamma / \delta_{vci}]$  TF must be

$$\frac{\gamma}{\delta_{vci}} = \frac{K_{vci}}{S} \frac{g}{V_G} \frac{\omega^2}{S^2 + 2\zeta \omega S + \omega^2} \quad (4.3)$$

Here  $V_G$  is the groundspeed. This  $[\gamma / \delta_{vci}]$  TF can be realized by using feed the forward gains  $K_{FFP}$  and  $K_{FFI}$  to create two zeros designed to cancel two poles of the  $[\gamma / \gamma_c]_{auto}$  TF, equation (3.3). One of these numerator zeros is used to cancel the  $\tau_{\theta_2}$  associated pole and the second zero is used to cancel the first order pole that is part of the third order part of the denominator of the  $[\gamma / \gamma_c]_{auto}$  TF. Thus the “ideal” SP frequency and damping coefficient in (4.1) can be specified. For example: selecting  $\omega = \omega_{SP} = 2$  rad/sec and  $\zeta = \zeta_{SP} = 1$  results in :

$$\frac{\gamma}{\delta_{vci}} = \frac{K_{vci}}{S} \frac{g}{V_G} \frac{(K_{FFP} \cdot S^2 + K_{FFI} \cdot S + 1)}{(.25S^2 + 1S + 1)(\tau_D S + 1)(\tau_{\theta_2} S + 1)} \quad (4.4)$$

The second order numerator of (4.4) must cancel the two first order poles. Therefore:

$$(K_{FFP} \cdot S^2 + K_{FFI} \cdot S + 1) = (\tau_D S + 1)(\tau_{\theta_2} S + 1) \quad (4.5)$$

However, to determine  $K_{FFP}$  and  $K_{FFI}$ ,  $\tau_D$  must be known, or one of the feedback gains must be known.

The simplest way is to select  $\tau_D$ . Then from (4.5) it follows that  $K_{FFP} = \tau_D \cdot \tau_{\theta_2}$  and  $K_{FFI} = \tau_D + \tau_{\theta_2}$ .

For example for  $\tau_D = 1$ , it follows that  $K_{FFP} = \tau_{\theta_2}$  and  $K_{FFI} = 1 + \tau_{\theta_2}$ . Also the following identity must hold:

$$(.25S^2 + 1S + 1)(\tau_D S + 1) = [\{1 / (K_q K_{\theta} K_{EI})\} S^3 + \{1 / (K_{\theta} K_{EI})\} S^2 + \{1 / (K_{EI})\} S + 1] \quad (4.6)$$

The right hand part of equation (4.6) is the third order part of the original  $[\gamma / \gamma_c]_{auto}$  TF, Equation (3.3).

For  $\tau_D = 1$  the gains become  $K_q = 5$  (rad/sec<sup>2</sup>)/(rad/sec),  $K_{\theta} = 1.6$  (rad/sec)/rad and  $K_{EI} = .5$  rad/rad. The gain  $K_{EI} = .5$  adequately supports the outerloop altitude and airspeed modes bandwidth of .1 rad/sec. The  $\gamma$  response lag relative to  $\gamma_c$  becomes  $\tau_{\gamma} = 1$  second.

The above sketched approach for designing the  $[\gamma / \gamma_c]_{auto}$  and  $[\gamma / \delta_{vci}]$  TF allows a quick evaluation of the change in the  $[\gamma / \gamma_c]_{auto}$  dynamics and the gains, in particular  $K_q$  and  $K_{EI}$ , for other choices of  $\tau_D$ . Here it was assumed that the linear elevator control actuator transfer function will have its lowest first order pole located at -20 rad/sec or higher. This allows for a gain  $K_q$  up to 5(rad/sec<sup>2</sup>)/(rad/sec) or somewhat higher, while still assuring that the lowest frequency pole of the actuator dynamics will not couple with the first order pole associated with the  $K_q$  control loop, to form a lowly damped oscillatory mode. The selected gains also allows for the addition of structural mode filters, if needed. The robustness margins can be increased further by increasing  $\tau_D$  which lowers  $K_q$ , but reduces  $K_{EI}$ . If the “ideal response model” is different than the one defined by equation (4.1), or if it needs to change for different flight conditions, it is a simple matter to recalculate the corresponding gains. More details on this FPA based Augmented Manual control mode design can be found in [3,4].

## Augmented Manual Mode – Thrust Control

No changes to the basic thrust control channel are required for the Augmented manual mode, except the feed forward gains  $KT_{FFP}$  and  $KT_{FFI}$  (implemented analogous to  $K_{FFP}$  and  $K_{FFI}$ ) can be used to minimize speed deviations due to vertical maneuvering. However,  $K_{FFP} = 0$  was found to relax throttle response during vertical stick inputs, albeit at the expense of incurring a slightly larger speed error.

## Pilot Display Requirements for manual $\gamma$ -control loop closure

The FPA-based augmented manual control mode was designed to meet the classical handling qualities requirements intended for pitch attitude control, so a standard Primary Flight Display can be used for closing the pilot control loop using pitch attitude. However, to realize “direct FPA Control” requires the addition of the FPA information to the PFD. In the earlier NASA “Velocity Vector Control” development program [5] it was found that  $\tau_\gamma = 1$  second, although less than for the unaugmented airplane, it is still too large for the pilot to be able to close the loop on  $\gamma$  directly. Therefore a quickened  $\gamma$  display signal must be used. The obvious candidate signal is  $\gamma_c$ . Pilot control loop closure around  $\gamma_c$ , instead of around the actual airplane dynamics, was found to work very well, since only 90 degrees lag is incurred in this loop, discounting the pilot’s lag. So then the pilot can use very high gain without PIO risk. To avoid displaying both  $\gamma$  and  $\gamma_c$ , a blended  $\gamma_{quick}$  signal can be used that responds like  $\gamma_c$  during maneuvering and reverts to  $\gamma$  when the pilot is out of the control loop. It is based on equation (4.3):

$$\gamma_{quick1} = \gamma + \frac{(1/\omega^2)S^2 + (2\zeta/\omega)S}{(1/\omega^2)S^2 + (2\zeta/\omega)S + 1} \gamma_c \quad (4.7)$$

or, by defining  $\tau_q = (2\zeta/\omega)$  a first order approximation of (4.11) becomes:

$$\gamma_{quick2} = \gamma + \frac{\tau_q S}{\tau_q S + 1} \gamma_c \quad (4.8)$$

Still another approach to “on demand”  $\gamma$  quickening was proposed in [6]. It adds a pitch rate signal to  $\gamma$ .

## Augmented Manual Mode – Envelope Protection

**Speed Envelope Protection.** The FPA-based augmented manual control mode should normally be operated with the autothrust engaged because of the lack of speed stability at constant throttle setting. However the airspeed should be allowed to drift after the thrust reaches the upper or lower limit and the pilot commands a  $\gamma$  in excess of the airplane’s steady state performance capability, or during maneuvering with the autothrust disengaged, as long as Vmin and Vmax protection is provided when the airplane’s excess kinetic energy runs out. Therefore simple independent Vmin, and Vmax control functions have been developed that work as follows. **When the autothrust is engaged**, the Vmin control function is armed to allow engagement using **SoECP** after the thrust-command reaches Tmax and after the Vmin control develops a pitch command that is more nose down than the pitch command developed by the manual FPA control. Likewise, the Vmax control function is armed to allow engagement using **SoECP** after the thrust-command reaches Tmin and after the Vmax control develops a pitch command that is more nose up than the manual FPA control. Also, the Vmin target is lowered in proportion to the nose up  $\delta_{vci}$  deflection, from the command speed at zero  $\delta_{vci}$  deflection to  $1.05V_{stall\phi}$  for full nose up deflection. Likewise, the Vmax target is increased in proportion to the nose down  $\delta_{vci}$  deflection, from the command speed at zero  $\delta_{vci}$  deflection to Vmo/Mmo + XX knots for full nose down deflection. **When the autothrust is disengaged**, the Vmin/Vmax envelope protection function is always armed to engage. In this case the Vmin target is  $1.2V_{stall\phi}$  at zero  $\delta_{vci}$  deflection. The Vmin target is lowered in proportion to the nose up  $\delta_{vci}$  deflection to  $1.05V_{stall\phi}$  for full nose up deflection. Here  $V_{stall\phi} = V_{stall1g} \sqrt{1/\cos\phi}$  is the stall speed for the airplane in a level coordinated banked turn. Likewise, the Vmax target is increased in proportion to the nose down  $\delta_{vci}$  deflection, from Vmo/Mmo at zero  $\delta_{vci}$  deflection to Vmo/Mmo + XX knots for a full nose down deflection.

**Normal Load Factor control.** To prevent excessive positive  $n_z$  that can result in stall or undesirable negative  $n_z$ , both a bank angle command limit and a full  $\delta_{vci}$  deflection  $n_z$  - command limit are imposed. The vertical maneuver authority,  $(n_{z_v})_{\max}$ , is calculated according to equation (4.9) below, and the NLF-command is scheduled so that a full vertical control inceptor deflection always commands the maximum safe NLF. However, it was found that simple command limiting cannot prevent exceeding the NLF limits for extreme stop to stop vertical inceptor deflections at high speed (e.g. due to PIO). Therefore a simple innerloop feedback NLF-limit control function was also implemented. A more detailed discussion on Envelope Protection requirements and design for automatic and augmented manual control mode can be found in the companion paper [4].

## Scheduling of the Command Gain, $K_{vci}$

To minimize the possibility of overstressing or stalling the airplane, the vertical control inceptor command gain  $K_{vci}$  needs to be scheduled as a function of stick deflection and airspeed, such that full vertical stick deflection commands the maximum safe Normal Load Factor ( $n_z$ ), at any speed. At speeds greater than the Maneuver Speed  $n_{z_{authority}} = n_{z_{structLim}}$ . Generally at design weight,  $n_{z_{structLim}} = 2.5$ . Below the Maneuver Speed  $n_{z_{authority}} = n_{z_{aeroLim}} = V^2 / V_{stall}^2 g$ . The vertical control inceptor deflection ( $\delta_{vci}$ ) is normalized to +1 for full nose up deflection and -1 for full nose down deflection. For  $\delta_{vci} = 1$  The maximum available normal load factor for vertical maneuvering,  $(n_{z_v})_{\max}$ , is:

$$(n_{z_v})_{\max} = n_{z_{authority}} - \Delta n_{z_\phi} - \Delta n_{z_{stallMargin}} \quad (4.9)$$

In equation (4.10)  $n_{z_{authority}}$  is the lower of  $n_{z_{structLim}}$  or the  $n_{z_{aeroLim}}$ ;  $\Delta n_{z_\phi} = (1/\cos\phi) - 1$  is the incremental load factor due to roll angle, assuming a coordinated turn;  $\Delta n_{z_{stallMargin}}$  is a selected safety margin, typically equal to .1. For this study it was decided that the negative  $n_z$  control authority should be limited to  $(n_{z_v})_{\min} = 0$ , rather than  $(n_{z_v})_{\min} = -1$ , because a capability to command  $(n_{z_v})_{\min} = 0$  in a vertical maneuver gives plenty maneuver authority for a transport airplane and protects the passengers and the airplane against possible injuries and damage. (An arrangement should be provided to change this limit to  $(n_{z_v})_{\min} = -1$  in case the airplane becomes inverted, since the airplane must remain controllable at any attitude.) Thus, with the  $n_{z_c}$  defined at three points for  $\delta_{vci} = 1, 0, -1$ , the above requirements can be met by defining the incremental normal load factor ( $\Delta n_{z_{cv}}$ ), commanded as a function of  $(n_{z_v})_{\max}$  and  $\delta_{vci}$ , using the following parabolic schedule:

$$\Delta n_{z_{cv}} = [\{.5(n_{z_v})_{\max} - 1\} \cdot \delta_{vci} + .5(n_{z_c})_{\max}] \cdot \delta_{vci} = K_{vci} \cdot \delta_{vci} \quad (4.10)$$

Therefore:

$$\dot{\gamma}_c = \Delta n_{z_{cv}} \cdot g / V_G = K_{vci} \cdot \delta_{vci} \cdot g / V_G \quad (4.11)$$

Here  $\Delta n_{z_{cv}}$  is the incremental load factor commanded by the vertical control inceptor deflection. It should be noted that for this schedule the command gradient,  $(\Delta n_{z_{cv}} / \delta_{vci})_{\delta_{vci}=0} = .5(n_{z_v})_{\max}$ , is a function of airspeed and the inceptor deflection. When combined with a passive inceptor that has a fixed force gradient, it produces a “stick force per g” ( $F_{vci} / \Delta n_{z_{cv}}$ ) that at high speeds decreases with increasing deflection and this is generally regarded as unacceptable for handling qualities. Another stick command schedule that allows for a selectable command gradient,  $(\Delta n_{z_{cv}} / \delta_{vci})_{\delta_{vci}=0} = grad$ , can be defined using



a (1-cos) function and the requirements: for  $\delta_{vci} = 1$   $\Delta n_{z_{cv}} = (n_{z_v})_{\max} - 1$ ; for  $\delta_{vci} = 0$   $\Delta n_{z_{cv}} = 0$ ; and for  $\delta_{vci} = -1$   $\Delta n_{z_{cv}} = -1$ . Then for  $\delta_{vci} \geq 0$  the relationship becomes:

$$\Delta n_{z_{cv}} = \delta_{vci} \cdot grad + \{(n_{z_v})_{\max} - 1 - grad\} [1 - \cos\{\delta_{vci} \cdot (\pi / 2)\}] \quad (4.12)$$

and for  $\delta_{vci} < 0$  the relationship becomes:

$$\Delta n_{z_{cv}} = \delta_{vci} \cdot grad + (-1 + grad) \cdot [1 - \cos\{\delta_{vci} \cdot (\pi / 2)\}] \quad (4.13)$$

Although for this command the gradient at zero control effector deflection can be selected, at high speed the  $F_{vci} / \Delta n_{z_{cv}}$  gradient still decreases with increasing deflection. So this schedule may also be unsuitable for use with a passive control inceptor that has a fixed force/deflection gradient. Still another alternative is to use a constant command gradient,  $(\Delta n_{z_{cv}} / \delta_{vci})$ , at any deflection and airspeed. This approach would produce a constant  $F_{vci} / \Delta n_{z_{cv}}$ , when using a passive constant force gradient control inceptor, but it also has a number of design and handling qualities issues. These include: matching full deflection command with maximum maneuver authority; unequal maximum positive and negative deflection; command gradient discontinuity around zero inceptor deflection and possibly for large nose up deflection; and possible need for flat zones where  $\Delta n_{z_{cv}} / \delta_{vci} = 0$ , used to prevent exceeding  $(n_{z_v})_{\max}$ . For these reasons, the FAA is currently sponsoring research to define design guidelines and certification requirements for passive and active control inceptor command gain and feel force gradient.

## Control Anticipation Parameter (CAP) Requirement

The CAP is defined as the ratio  $\ddot{\theta}_{t=0} / \Delta n_{z_{t=\infty}}$ . From the  $[\gamma / \delta_{vci}]$  TF defined by (4.5), it follows that:

$$\ddot{\theta}_{t=0} = \delta_{vci} \cdot K_{vci} \cdot (g / V_G) \cdot K_{FFP} \cdot K_{EI} \cdot K_{\theta} \cdot K_q \quad (4.15)$$

For a constant stick input the final incremental load factor is:

$$(\Delta n_{z_c})_{t=\infty} = (V_G / g) \dot{\gamma}_c = (V_G / g) \cdot \delta_{vci} \cdot K_{vci} \cdot (g / V_G) \quad (4.16)$$

Therefore  $CAP = (g / V_G) \cdot K_{FFP} \cdot K_{EI} \cdot K_{\theta} \cdot K_q \quad (4.17)$

Thus, for an approach condition with  $V = 215$  ft/sec and  $\tau_{\theta_2} = 2$  and a selected  $\tau_{\gamma} = 1$ , it follows that the required value  $K_{FFP} = \tau_{\theta_2} = 2$ , resulting in  $CAP = 1.2$ . This is well within the .28 to 3.6 CAP range allowed in MIL-STD-1757A for level 1 handling qualities. With the feedback gains  $K_{EI}$ ,  $K_{\theta}$  and  $K_q$  pre-determined, the only parameter that can change CAP is  $K_{FFP}$ . However,  $K_{FFP}$  is a critical design parameter that cannot be varied much from the calculated value in the above analysis and still achieve acceptable responses. Furthermore, to achieve harmony between the initial pitch acceleration and the final  $n_z$  response  $K_{FFI}$  (here controlling the steady state  $n_z$  lag relative to  $\delta_{vci} \cdot K_{vci} / S$  must be selected within a narrow range, to achieve the desired value of  $\tau_{\gamma}$ . Another way to analyze CAP is to look the variation of CAP as a function of  $\tau_D$ . Changing  $\tau_D$  has no effect on the final  $[\gamma / \delta_{vci}]$  TF, nor does it change the product  $K_{EI} \cdot K_{\theta} \cdot K_q$ , but  $K_{FFP}$  varies in proportion to  $\tau_D$ , so it is possible to change CAP value without changing the  $[\gamma / \delta_{vci}]$  response! One more observation: for higher values of  $\tau_D$  the basic  $[\gamma / \gamma_c]_{auto}$  TF incurs more lag, because it reduces  $K_{EI}$  (see equation 3.5), so in order to still achieve the same final  $\gamma / \delta_{vci}$  response, the feed forward gains and  $K_{FFI}$  increase to compensate for the increased lag. So then the control augmentation relies more on the  $K_{FFP}$  direct feed through signal path to the

elevator and less on the feedback control signal paths. Conclusion: CAP is a dubious Handling Quality criterion that may need further updates or replacement.

## FPA based Augmented Manual Control Simulation Results

The same simulation as used above for the automatic modes was used to generate the time responses below for the FPA-based Augmented Manual control mode as defined above. Figure 4.3 (left plot) shows the responses to  $\delta_{stick_{pitch}} = .1$ , starting at  $t=20$  second for a duration of 5 seconds, resulting in a change of flight path angle of  $\sim 2$  degrees. The responses are very smooth, without an overshoot of the  $\gamma_c$ , or oscillations. Note the responses in Angle of Attack (AOA) and NLF ( $n_z$ ) are also controlled very smoothly.

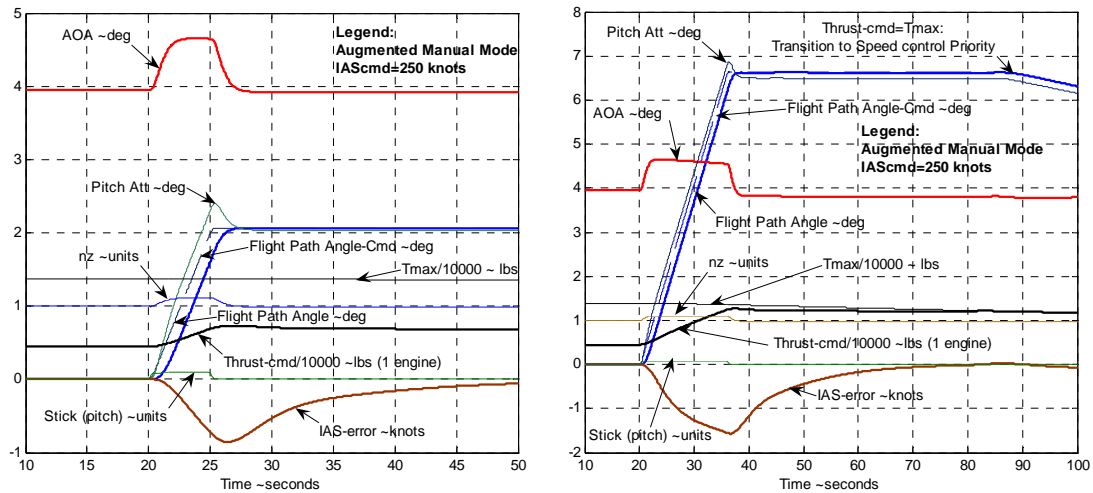


**Figure 4.3 FPA-based Augmented Manual Mode: responses to  $\delta_{vci} = .1$**

The flight path angle response lag is as designed:  $\tau_\gamma = 1$  second. The pitch attitude shown is biased by the amount of the trim pitch attitude before the maneuver starts, to show its lead relative to lead  $\gamma_c$ .

The pitch attitude Att leads the  $\gamma$ -response by  $\tau_{\theta_2}$  and causes the attitude to drop back when the control inceptor is released, if  $\tau_{\theta_2} > 1$ . The IAS-error remains less than 1knot. The thrust command does not reach

Tmax. Figure 4.3 (right plot) shows the responses to  $\delta_{vci} = .1$ , starting at  $t=20$  second for a duration of 16 seconds, resulting in a change of flight path angle of  $\sim 6.6$  degrees. During this maneuver the thrust command increase to within a small margin of Tmax. The IAS-error reaches a maximum of  $\sim 1.5$  knot and then gradually reduces to  $\sim$ zero. Then, as Tmax decreases with increasing altitude, the thrust command reaches Tmax at  $t=87$  seconds and this causes a reversion from **PoECP** to **SoECP**, in order to maintain the airspeed. At that point the flight path angle will start to fall off in proportion to the thrust fall off.

Figure 4.4 (left plot) shows the responses to  $\delta_{vci} = .1$ , starting at  $t=20$  second held indefinitely. This causes the flight path angle to rise until the Vmin control engages (using **SoECP**), a short time after the thrust command reaches Tmax. At that point the flight path angle reaches  $\sim 9$  degrees, then starts to decline as a result of the Vmin control priority. As discussed above, the Vmin control has been designed to mimic speed stability, allowing a final speed deviation in proportion to the  $\delta_{vci}$  deflection. So in the left plot, the speed bleeds of 10 % of the speed margin to  $1.05V_{stall}$ . In the Figure 4.4 (right plot) a full nose up deflection is applied ( $\delta_{vci} = 1$ ). This results in a very aggressive maneuver using all available NLF

authority. For this case, the thrust command very quickly reaches  $T_{max}$  and  $V_{min}$  control priority is established very shortly before the NLF and the AOA reach their peak value, at  $\sim 2.2$  and 13 degrees respectively. The stall AOA is 15 degrees. The flight path angle reaches a peak value of  $\sim 22$  degree. The real peak pitch attitude reached is  $\sim 38$  degrees (34 degrees as shown + 4 degrees trim value before the start of the maneuver). The final speed settles at  $1.05V_{stall}$ . The control responses and reversion to  $V_{min}$  control are very smooth and without transients.

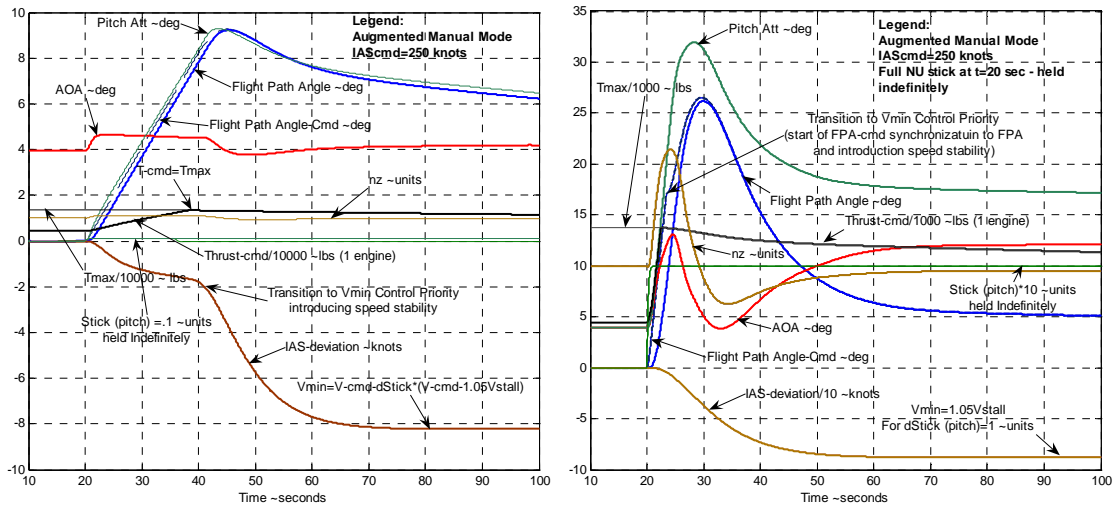


**Figure 4.4 FPA-based Augmented Manual Mode, left: responses to  $\delta_{vci} = .1$  held indefinitely; right:  $\delta_{vci} = 1$ , held indefinitely**

## 7 Additional TECS & THCS related developments

**Ecological PFD.** The TECS energy based control strategy and the THCS Heading control strategy can be embedded into the Primary flight Display (PFD), to bring out control guidance cues for using manual Thrust, Pitch and Roll control to efficiently and simultaneously capture and track airspeed, Altitude and heading targets in an energy efficient exponential and overshoot-free manner. This enhanced Ecological PFD concept is summarized in the companion paper [3] and described in more detail in [8].

**TECS/THCS Mode Control Panel.** In order for the pilot to be able to use one mental model for all FG&C operations and to minimize effort needed for reuse, the TECS & THCS designs use one generalized guidance and control strategy for all automatic and augmented manual control modes. For the same reason this strategy has also been applied to the design of the FG&C Mode Control Panel (MCP) and Flight Mode Annunciation (FMA) function on the PFD. These developments are described in the companion paper [3].

**Interactive Real-Time TECS/THCS Demonstration System.** An interactive Real-Time TECS/THCS Demonstration System was developed, using The Simulink Real Time Workshop program, including the twin engine transport airplane simulation, an interactive TECS/THCS Mode Control Panel with integrated Controller Pilot Data link Communication functions, a joystick manual control capability and several versions of Primary Flight Displays including a Flight Mode Annunciation Panel.

## 8 Conclusion

This paper describes recent design enhancements of the Total Energy Control System (TECS). TECS uses a “pilot like” MIMO energy-based guidance and control strategy to generalize and functionally integrate all

automatic and augmented manual control modes for airplane control in the vertical plane. This design strategy enables the pilot to use one mental model for all FG&C operations. It also minimizes the effort needed for design application on various airplane programs. To limit the scope of this paper, additional related subject matter is covered in two companion papers [3] and [4]. Companion paper [3] covers design updates to the Total Heading Control System (THCS), the enhanced ecological PFD [also called Energy Management PFD (EMPFD)], and the design of the Mode Control Panel and the Flight Mode Annunciation Panel. THCS uses strategies analogous to TECS, to generalize and functionally integrate all automatic and augmented manual lateral-direction control modes. TECS and THCS provide full 6 degrees of freedom airplane control capability to the limits of the safe flight envelope, without allowing LOC by departure outside the safe flight envelope. It eliminates stand alone SISO based Autothrottle, Yaw Damper/ Turn Coordination and Trust Asymmetry Compensation systems. The EMPFD incorporates the TECS and THC guidance strategies to enhance pilot awareness of airplane maneuver capabilities and provide guidance cues to use the controls in an effective and energy efficient manner. A second companion paper [4] discusses various options for designing flight envelope protection functions.

## 9 References

1. A.A. Lambregts: “Vertical Flight Path and speed Control Autopilot design Using Total Energy principles”, AIAA 83-2239CP
2. A.A. Lambregts: “Automatic Flight Controls Concepts and methods”, Koninklijke Nederlandse Vereniging voor Luchtvaart, Jaarverslag, 1996
3. A.A. Lambregts: “THCS Generalized Airplane Control System Design”, 2013 CEAS conference on Guidance, Navigation and Control, Delft, The Netherlands
4. A.A. Lambregts: “Flight Envelope Protection Strategies for Automatic and Augmented Manual Control”, 2013 CEAS conference on Guidance, Navigation and Control
5. A.A.Lambregts and D.G.Cannon: “Development of a Control Wheel Steering Mode and Suitable Displays that Reduce Pilot Workload and Improve Efficiency and Safety of Operation in the Terminal Area and in Windshear”, AIAA G&C paper 79-1887
6. A.A. Lambregts: “Fundamentals of Fly-By-Wire Augmented Manual Control”, SAE 05WAC-62
7. D. Niedermeier, A.A. Lambregts: “Design of an Intuitive Flight Control System”, 2009 CEAS Conference
8. R. Bray: “A Head-Up Display Format for Transport Aircraft Approach and Landing”, NASA TM-81199, July 1980; NASA HUD Report 11; N80-29295
9. A.A. Lambregts, R. Rademaker, E. Theunissen: “A New Ecological Primary Flight Display Concept”, DASC 2008